RESEARCH PAPER

Enhancing cellulose hydrolysis via cellulase immobilization on zeolitic imidazolate frameworks using physical adsorption

Liqun Sun[1,2] · **Chaozhong Xu**[1,2] · **Shanshan Tong**[1,2] · **Xiaoli Gu**[1,2]

Abstract

This study investigates the immobilization of cellulase on zeolitic imidazolate frameworks (ZIFs) by physical adsorption, specifically the ZIF-8-NH_2 and Fe_3O_4@ZIF-8-NH_2, to enhance enzymatic hydrolysis efficiency. The immobilization process was thoroughly analyzed, including optimization of conditions and characterization of ZIF carriers and immobilized enzymes. The impacts on the catalytic activity of cellulase under various temperatures, pH levels, and storage conditions were examined. Additionally, the reusability of the immobilized enzyme was assessed. Results showed the cellulase immobilized on Fe_3O_4@ZIF-8-NH_2 exhibited a high loading capacity of 339.64 mg/g, surpassing previous studies. Its relative enzymatic activity was found to be 71.39%. Additionally, this immobilized enzyme system demonstrates robust reusability, retaining 68.42% of its initial activity even after 10 cycles. These findings underscore the potential of Fe_3O_4@ZIF-8-NH_2 as a highly efficient platform for cellulase immobilization, with promising implications for lignocellulosic biorefinery.

Keywords Cellulase immobilization · Physical adsorption · Zeolitic imidazolate frameworks · Magnetic nanoparticles · Amino-functionalization

Introduction

At present, the demand for energy is growing rapidly, and the instability of fossil resources and global climate change have become increasingly prominent. Human beings urgently need to find renewable resources that can replace fossil resources. Therefore, the production of biofuels, biochemicals, and biomaterials through lignocellulosic biorefinery using biomass as raw materials has become a globally focused research area. Lignocellulosic biomass is obtained from inedible crops and other wastes. Then, it is decomposed into simpler and shorter polysaccharide chains by biological, chemical, or physical methods. Once cellulose and hemicellulose are separated by pretreatment, the next major goal is to hydrolyze these polymers with enzymes. Cellulases are used to break down short chains of polysaccharide cellulose to form glucose, which can then be fermented to form biofuels, such as bioethanol. However, this process is not economical because cellulases account for about 50% of the total hydrolysis cost [1]. Therefore, it is crucial to use a cost-effective process and develop sustainable routes to ensure the recycling and reuse of cellulases [2, 3].

Currently, many studies focus on the process of immobilized cellulase, a method of immobilizing cellulase to carriers using physical adsorption or chemical crosslinking. The immobilization of cellulase can effectively enhance the utilization rate of cellulase and increase its stability. Moreover, it enables the recycling and reuse of cellulase. For example, Lima et al. found the immobilized cellulase on magnetic nanoparticles exhibited broader temperature stability and

Liqun Sun and Chaozhong Xu contributed equally to this work.

✉ Chaozhong Xu
xucz@njfu.edu.cn

✉ Xiaoli Gu
guxiaoli@njfu.edu.cn

Liqun Sun
s1325336878@outlook.com

Shanshan Tong
tss@njfu.edu.cn

1 Jiangsu Co-Innovation Center of Efficient Processing and Utilization of Forest Resources, College of Chemical Engineering, Nanjing Forestry University, Nanjing 210037, People's Republic of China

2 Jiangsu Key Lab of Biomass-Based Green Fuels and Chemicals, Nanjing 210037, People's Republic of China

great reusability, maintaining 69% of the initial enzyme activity after eight cycles of use [4]. Andriani et al. immobilized cellulase using bacillus subtilis TD6, with immobilized cellulase showing storage stability at 4 °C for up to 12 days [5]. Lima et al. found cellulase immobilized on kaolin allowed for efficient recovery and reuse of the enzyme [6]. Ungurean et al. studied the use of binary or ternary mixtures of tetramethoxysilane (TMOS) and alkyl or aryl substituted trimethoxysilane as precursors to immobilize cellulase from *Trichoderma reesei* by sol–gel encapsulation, resulting in 92% recovery of total enzymatic activity, with 40% retention of the initial activity after five batch hydrolysis cycles [7].

An increasing number of researchers are exploring the use of metal–organic frameworks (MOFs) as carriers for cellulase immobilization. Due to their adjustable structure, high porosity, large surface area, and abundant binding sites, MOFs are considered as novel carriers for immobilizing cellulase. Xie et al. prepared two MOF-cellulase composites by physical adsorption, demonstrating improved thermal stability, pH tolerance, and lifespan of immobilized cellulose [8]. Similarly, Qi et al. investigated cellulase immobilization on core–shell MOF structures, where magnetic UiO-66-NH$_2$ immobilized cellulase through glutaraldehyde crosslinker showed superior performance in pH stability, thermal stability, and catalytic efficiency compared to its free form [9].

Currently, more research is inclined towards using magnetic MOF materials for enzyme immobilization, primarily because magnetic MOFs allow for the simple and rapid separation of immobilized enzymes from reaction mixtures using an external magnetic field. This eliminates the need for centrifugation or filtration, significantly reducing process time and cost, and facilitating enzyme recovery and reuse. The incorporation of magnetic nanoparticles can further increase the surface area available for enzyme attachment, potentially improving enzyme loading capacities and catalytic efficiencies [10, 11].

Despite significant advancements in using MOFs to immobilize cellulase enzymes, these studies primarily employ covalent bonding or encapsulation methods for immobilization. While these approaches offer certain advantages, they also have clear disadvantages. For instance, covalent bonding can improve stability and reduce enzymatic leakage during hydrolysis but it requires complex immobilization procedures and reaction conditions. Additionally, the covalent bond formation may involve reactions with the protein's active site, potentially disrupting the natural structure of cellulase and reducing enzyme activity, thereby compromising the stability and reusability of the immobilized enzyme system. On the other hand, encapsulation, which confines enzymes within a matrix, can protect the enzymes from harsh catalytic conditions. However, the matrix or capsule can impede substrate-enzyme contact through mass transfer limitations, thus reducing overall catalytic efficiency.

In practical applications, the stability and catalytic efficiency of cellulase are crucial; therefore, it is necessary to explore alternative immobilization methods and carriers [12–15].

This study synthesized ZIF-8-NH$_2$ and further modified it using magnetic nanoparticles, using adsorption for the immobilization of cellulase. The immobilization conditions were optimized, and the physicochemical properties of the immobilized enzyme were characterized. The study found that immobilizing enzymes through adsorption effectively preserves enzyme activity, enhances stability, improves hydrolysis efficiency, and maintains usability after multiple hydrolysis cycles. This research will contribute to the efficient and cost-effective conversion of lignocellulosic biomass, thereby advancing the fields of biofuels and biorefining.

Materials and methods

Materials

Cellic CTec2 cellulase, possessing a filter paper activity rate of 197.55 FPU/mL, was procured from Sigma. Additionally, essential chemicals for the experiments, including zinc nitrate hexahydrate (Zn(NO$_3$)$_2$·6H$_2$O), 2-methylimidazole (Hmim), 2-aminobenzimidazole, ferric chloride (FeCl$_3$), methanol, sodium acetate, sodium citrate, and microcrystalline cellulose (MCC) were sourced from Aladdin.

Preparation of ZIF carriers

ZIF-8-NH$_2$

For the synthesis of ZIF-8, a solution was prepared by dissolving 2.975 g (10 mmol) of Zn(NO$_3$)$_2$·6H$_2$O, 6.240 g (76 mmol) Hmim, and 0.532 g (4 mmol) 2-aminobenzimidazole in 100 mL of methanol. The solution was stirred for 2 h, followed by a resting period of 6 h for precipitation. The supernatant was then discarded, and the precipitate was cleansed thrice using methanol and water before being vacuum-dried at 60 °C for 12 h.

Fe$_3$O$_4$@ZIF-8-NH$_2$

Magnetite nanoparticles were synthesized via solvothermal method. To begin, 3.9 gFeCl$_3$ and 1.2 g anhydrous sodium citrate were dissolved in 60 mL of ethylene glycol, followed by the addition of 1.2 g anhydrous sodium acetate to form a yellow solution. This solution was then transferred to a high-pressure autoclave and heated at 200 °C for 10 h. After cooling, the black particles were washed three times with deionized water and then dried under vacuum at 60 °C for 12 h [16].

To prepare Fe_3O_4@ZIF-8-NH_2, 2.975 g (10 mmol) of $Zn(NO_3)_2 \cdot 6H_2O$ and 1.1835 g of magnetite were ultrasonicated in 100 mL of methanol for 1 h. Subsequently, 6.240 g (76 mmol) of Hmim and 0.532 g (4 mmol) of 2-amino benzimidazole were introduced into the mixture and stirred at room temperature for 1.5 h. The resulting mixture was then centrifuged, washed three times with methanol and deionized water, and dried under vacuum to obtain magnetic ZIF-8-NH_2.

Cellulase immobilization on ZIF carriers by physical adsorption

A 20 mg sample of the ZIFs (ZIF-8-NH_2 and Fe_3O_4@ZIF-8-NH_2) was combined with cellulase in varying quantities within a 50 mM sodium citrate buffer (pH 4.8) to facilitate enzyme immobilization via physical adsorption. Following a 2 h immobilization phase, the mixtures were centrifuged to separate the supernatant from the precipitate, which was then washed until protein-free. The final immobilized product was vacuum-dried and stored at 4 °C for subsequent analysis.

The optimization of immobilization parameters for the ZIF constructs was conducted by evaluating enzyme loading capacities and activities under different conditions, including enzyme-to-carrier ratios (0.25 to 1.75 w/w).

Characterization of ZIF carriers and ZIF-immobilized cellulases

XRD

The crystalline structures and functional groups of both ZIFs and immobilized cellulase were characterized using XRD (Shimadzu XRD-6100, Japan), employing Cu-Kα radiation across a 5–40° scattering angle, under a 40 kV and 40 mA setting.

FTIR

The chemical compositions were assessed using FTIR (Thermo Nicolet NEXUS-670, USA), with each sample undergoing 64 scans in transmission mode, covering a 400–4000 cm^{-1} spectral range with a 2 cm^{-1} resolution.

SEM

The surface morphology was examined using SEM (Hitachi Regulus 8100, Japan), where samples were gold-coated to enhance conductivity prior to imaging.

BET

The specific surface area and porosity were quantified using nitrogen adsorption isotherms, analyzed via the BET method on a Micromeritics ASAP 2020 apparatus.

Determination of loading capacity and cellulase activity

Loading capacity

The protein content of cellulase in the initial solution before immobilization and in the supernatant after immobilization was estimated using the Bradford method [17], with bovine serum albumin as the standard protein. The loading efficiency of cellulase protein is calculated as follows:

$$\text{Loading capacity}(mg/g) = \frac{C_i V_i - C_s V_s - C_w V_w}{m_c}$$

where C_i and C_s C_w are the protein concentrations (mg/mL) of the initial cellulase solution and the supernatant, respectively. V_i and V_s are the volumes (mL) of the initial cellulase solution and the supernatant, respectively, and m_c is the mass of the carrier (g).

Cellulase activity

The activity of cellulase was measured using the filter paper enzyme activity method, referring to the NREL/TP-5 10–42628 standard method [18]. This method determines the dilution factor corresponding to the production of 2 mg of glucose under the action of cellulase at different dilutions, thereby calculating the filter paper enzyme activity of cellulase. The formula for calculating the activity of cellulase is as follows:

$$\text{Cellulase activity (FPU/mL)} = \frac{2.0mg/0.18(mg/\mu mol)}{0.5ml \times 60min} \times Dilution\,factor$$

The relative activity of immobilized cellulase is calculated as follows:

$$\text{Relative activity}(\%) = \frac{U_f}{U_i} \times 100\%$$

where U_i and U_f are the activities of cellulase before and after immobilization, respectively.

Study of the properties of free and ZIF-immobilized cellulases

Temperature stability

The stability of both immobilized and non-immobilized (free) cellulase across the range of temperatures (30 °C to 80 °C) was evaluated to determine the enzyme's thermal

tolerance. The assessment utilized the previously described methodology [19], employing a sodium citrate buffer at pH 4.8 for activity measurement.

pH stability

To examine how varying pH levels affect the catalytic efficiency of both immobilized and free cellulase, the study substituted the standard pH 4.8 sodium citrate buffer with buffers of pH values 3, 4, 4.8, 6, and 7. These tests were performed at a constant temperature of 50 °C.

Storage stability

The long-term stability of cellulase, both in its free and immobilized forms, was monitored over a 30-day period in a sodium citrate buffer (pH 4.8) at 4 °C. Activity levels were recorded every 5 days to evaluate and compare the preservation of enzymatic function in ZIF-immobilized enzymes versus their free counterparts.

Enzyme leaching

To quantify the extent of cellulase leaching from its immobilized state, experiments were set up where a predetermined quantity of immobilized cellulase was incubated in 50 mM sodium citrate buffer (pH 4.8) at 4 °C. The supernatant was collected every 2 days for protein concentration analysis to ascertain the degree of enzyme detachment from ZIF carriers.

Cellulose hydrolysis snd reusability of ZIF-immobilized cellulases

Cellulose hydrolysis

The degradation of microcrystalline cellulose (MCC) was executed by employing cellulase enzymes in a fixed and free form within a 50 mM sodium citrate buffer at pH 4.8. The MCC acted as the substrate at a 5% (w/w) concentration, with the enzyme introduced at a rate of 5 FPU/g of substrate. This enzymatic hydrolysis was performed in an incubating shaker set to 50 °C and 150 rpm, spanning a duration of 72 h. Periodic sampling was done at 12, 24, 48, and 72 h to measure the glucose yield. Glucose quantification was achieved through high performance liquid chromatography (HPLC, Agilent 1260, United States) utilizing a Bio-Rad Aminex HPX-87 H column (7.8 mm by 300 mm), operating at a 0.6 mL/min flow rate with 5 mM sulfuric acid serving as the eluent.

The hydrolysis yield is calculated as follows:

$$\text{Hydrolysis yield (\%)} = \frac{C_\text{p} V \times 0.9}{m_\text{S}} \times 100\%$$

where C_p is the concentration of glucose product (g/L), V is the volume of the hydrolysis system (mL), and ms is the mass of MCC substrate (g).

Reusability of ZIF-immobilized cellulases

To assess the recyclability, the enzymatic hydrolysis trials were conducted employing the ZIF-immobilized cellulases under the same conditions as mentioned above. The reaction was conducted at 50 ℃ for 30 min. After completion, the cellulases was separated by centrifugation and washed three times with buffer solution. The recovered cellulases was added to a new MCC solution. This process was repeated for 10 cycles under the same conditions. The activity of the immobilized enzyme was determined for each cycle.

Results and discussion

Characterization of ZIFs and ZIF-immobilized cellulases

As shown in Fig. 1, the XRD image reflects changes in the position and intensity of diffraction peaks. ZIF-8-NH$_2$ typically exhibits characteristic peaks at specific 2θ values, such as 7.3°, 10.3°, 12.7°, 16.4°, and 18.0°, corresponding to the (011), (002), (112), (022), and (013) planes, respectively. After modification with magnetic nanoparticles, the ZIF-8-NH$_2$ showed additional characteristic peaks at 30.2°and 35.5° besides the original peaks. This indicates that Fe$_3$O$_4$ has been successfully modified onto the carrier. The ZIF-immobilized cellulases showed minimal differences compared to the original ZIF carrier. This is because the cellulase does not possess a crystalline structure, and hence no additional characteristic peaks exist.

Figure 2 shows the FTIR spectra of the ZIF carrier and cellulase enzyme immobilized on ZIF. Typically, ZIF-8 materials exhibit a strong peak around 420 cm^{-1}, attributed to the stretching vibration of Zn-N bonds. Fe$_3$O$_4$@ZIF-8-NH$_2$ composite materials simultaneously exhibit characteristic peaks of both ZIF-8 and Fe$_3$O$_4$. There is a peak at 580 cm^{-1}corresponding to the Fe–O bond of Fe$_3$O$_4$. Another peak at 3300 cm^{-1} corresponds to the stretching vibration of the N–H bond [20]. Cellulase@ZIF-8 and cellulase@ZIF-8-NH$_2$ composite materials should exhibit both the characteristic peak of cellulase and the characteristic peak of the ZIF carrier after cellulase immobilization. For physical adsorption on ZIF-8-NH$_2$ and Fe$_3$O$_4$@ZIF-8-NH$_2$, the peaks characteristic of cellulase, such as amide I (C-O stretching) at around 1660 cm^{-1} and amide II (N–H bending
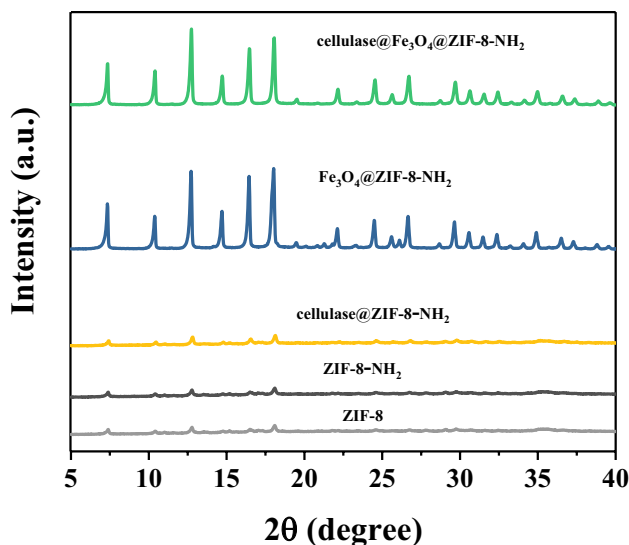
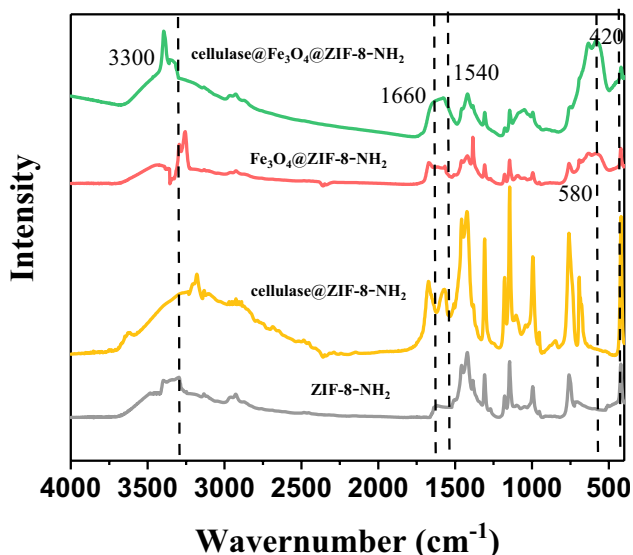**Fig. 1** XRD patterns of ZIF carriers and ZIF-immobilized cellulases

Fig. 2 The FTIR spectra of ZIFs and ZIF-immobilized cellulase

and C-N stretching) vibrations at approximately 1540 cm^{-1}, are observed. The presence of these additional peaks confirms the successful loading of cellulase onto the ZIF carriers [9, 21].

Figure 3 displays SEM images of the ZIF carriers and the ZIF carrier with immobilized cellulase. In Fig. 3a, b and e, it can be observed that ZIF-8 typically exhibits a rhombic dodecahedron shape, and ZIF-8-NH$_2$ exhibits an overall roughened rhombic dodecahedron shape after amino functionalization. Compared to ZIF-8-NH$_2$, Fe$_3$O$_4$@ZIF-8-NH$_2$ features a core–shell structure with Fe$_3$O$_4$ nanoparticles as the core and ZIF-8 as the shell. Due to the presence of -NH$_2$

groups, Fe$_3$O$_4$@ZIF-8-NH$_2$ also exhibits a similar rough surface. From Fig. 3c and d, it can be observed that enzyme molecules create small protrusions on the surface of ZIF materials after immobilization. Cellulase@ZIF-8-NH$_2$, due to the presence of -NH2 groups and cellulase molecules, displays an even rougher surface. Cellulase@Fe$_3$O$_4$@ZIF-8-NH$_2$, also due to the presence of amino groups and cellulase molecules, exhibits an even rougher surface.

As shown in Fig. 4, the adsorption isotherm of ZIF-8 and ZIF-8-NH$_2$ exhibits a type I curve, indicating its microporous structure. However, the adsorption isotherm of Fe$_3$O$_4$@ZIF-8-NH$_2$ displays a type IV curve, suggesting that the magnetic ZIF material possesses both microporous and mesoporous structures [22]. As seen in Table 1, the specific surface area of ZIF-8-NH$_2$ is 434.75 m^2/g, while that of Fe$_3$O$_4$@ZIF-8-NH$_2$ is 1166.86 m^2/g, and that of ZIF-8 is only 333.06 m^2/g. The larger specific surface area enables the MOF material to well absorb the cellulase Thus, Fe$_3$O$_4$@ZIF-8-NH$_2$ has a much larger surface area than ZIF-8-NH$_2$, indicating a stronger loading capacity.

Optimization of immobilization process parameters

Figures 5a and b demonstrate that under a 2 h immobilization time, different ratios of enzyme to carrier significantly affect the loading capacity and immobilized enzyme activity Generally, the loading capacity and activity of the enzyme first increase with the enzyme to carrier ratio, and then decrease. This may be due to the limited binding sites and loading capacity of the ZIF carrier. When reaching a maximum loaded protein, the tight and compact loading causes protein interactions and conformational changes [23]. Excessive enzyme can lead to aggregation, hindering the contact between the enzyme and the substrate, ultimately reducing loading capacity and relative enzyme activity. For ZIF-8-NH$_2$, the highest loading capacity and enzyme activity were observed at a ratio of 1.25, being 263.3 mg/g and 66.3%, respectively, while for Fe$_3$O$_4$@ZIF-8-NH$_2$, the maximum loading capacity and activity were achieved at a mass ratio of 1.5, amounting to 339.8 mg/g and 71.39%.

Comparison of the enzymatic properties of free and ZIF-immobilized cellulases

From Fig. 6a, it is observed that cellulase exhibits its highest activity at 50 °C [9, 24]. Once the reaction temperature exceeds the optimum value, the activity of the free enzyme sharply declines, with a loss of nearly 55% of its activity at 80 °C. In contrast, the cellulase immobilized on ZIF retains a good level of activity, suggesting enhanced thermal stability. This enhancement is likely due to the adsorption of cellulase onto the MOF, which strengthens the protein and restricts conformational changes during heating. Specifically, the
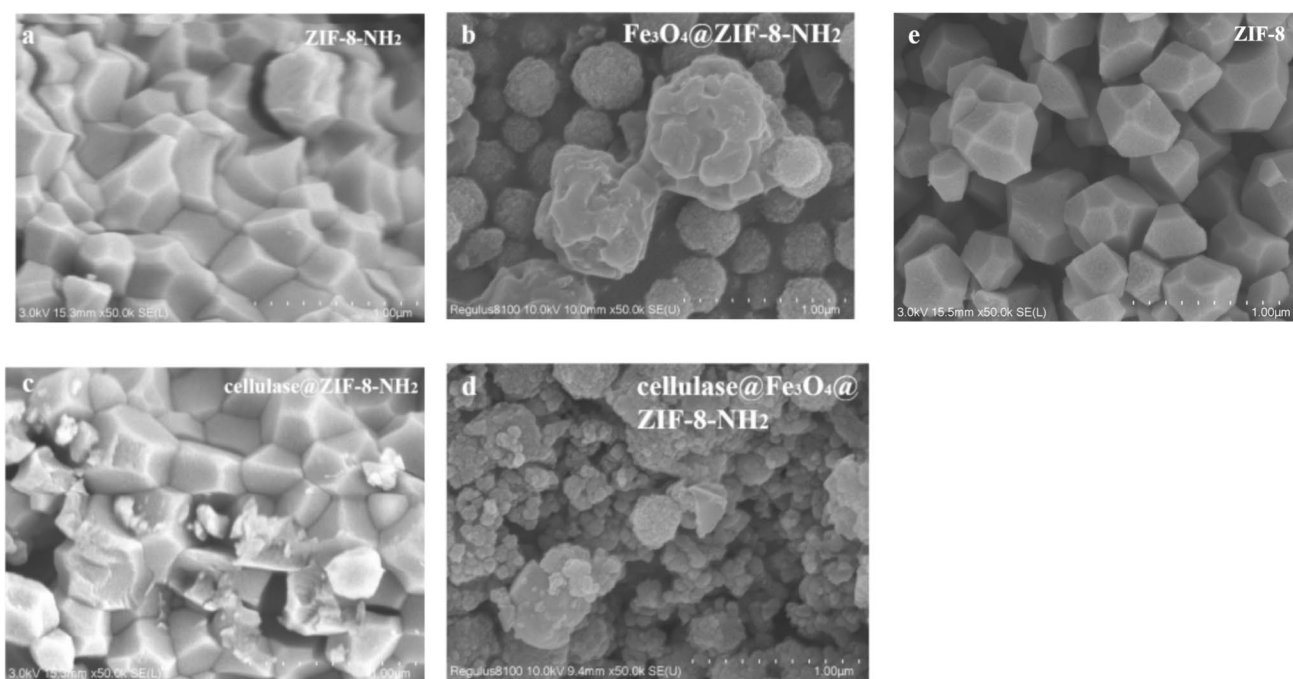
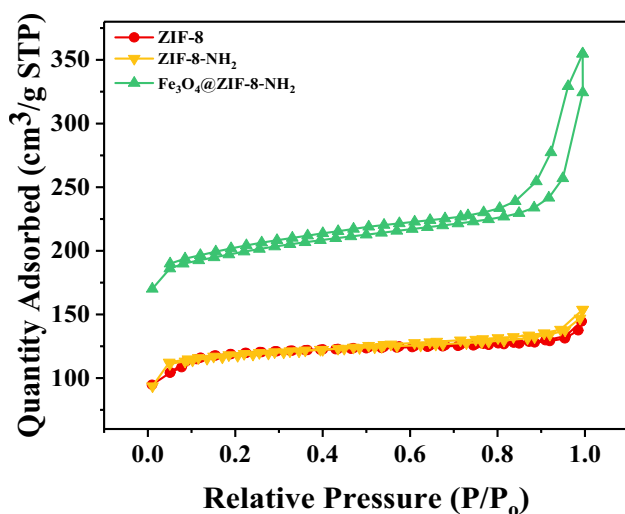**Fig. 3** SEM images of ZIF carriers and ZIF-immobilized cellulases

Fig. 4 Nitrogen (N2) sorption isotherms of ZIF carriers

Table 1 Specific Surface Area and pore characteristics of ZIF carriers and ZIF-immobilized cellulases

Carriers	BET Surface area(m²/g)	average pore size(nm)
ZIF-8	333.06	2.58
ZIF-8-NH₂	434.75	2.04
Fe₃O₄@ZIF-8-NH₂	1166.86	1.62

relative enzyme activities of ZIF-8-NH$_2$ and Fe$_3$O$_4$@ZIF-8-NH$_2$ at 80 °C are 71.8% and 82.1%, respectively, with Fe$_3$O$_4$@ZIF-8-NH$_2$ immobilized cellulase exhibiting even better thermal stability.

Figure 6b reveals that the pH tolerance of immobilized cellulase is higher than that of the free enzyme. For example, at pH 7, the relative residual enzyme activity of the free cellulase is only 42%, while it is 77% for ZIF-8-NH$_2$ immobilized cellulase and 80% for Fe$_3$O$_4$@ZIF-8-NH$_2$ immobilized cellulase. This improved tolerance might be due to changes in ionization behavior caused by immobilization on ZIFs, protecting the immobilized cellulase from pH-induced deactivation [8, 9].

From Fig. 6c, it is observed that the activity of free cellulase drops to 14% after 30 days, while the activities of cellulase immobilized on ZIF-8-NH$_2$ and Fe$_3$O$_4$@ZIF-8-NH$_2$ maintain at 59% and 65%, respectively. This stability could be attributed to the stable microenvironment provided by the ZIFs material, which helps protect the enzyme from external conditions. Additionally, the porous structure of ZIFs reduces enzyme aggregation, thereby minimizing deactivation [19]. The interaction between cellulase and the ZIF carrier reduces the impact of charged residues, enhancing the affinity of cellulase for the carrier. Therefore, cellulase immobilized on ZIF carriers exhibits better storage stability [25].

Figure 6d shows the leaching rates of cellulase immobilized on different ZIF carriers. Due to the reversible nature

Fig. 5 Effect of enzyme-to-support ratio on loading capacity and relative activity for different ZIF carriers
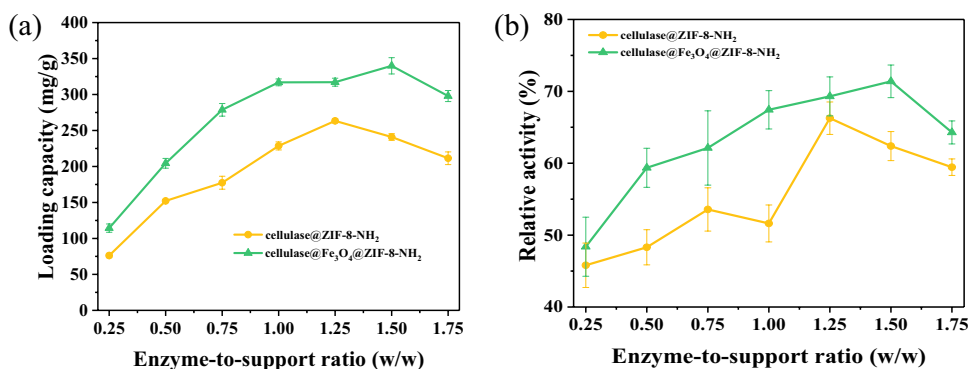
of adsorption, the leaching rates of ZIF-8-NH$_2$ and Fe$_3$O$_4$@ZIF-8-NH$_2$ within 10 days are 16.7% and 14.1%, respectively. The magnetically modified ZIF-8-NH$_2$ shows a lower leaching rate, likely due to its more stable core–shell structure, which reduces enzyme leakage.

Cellulose hydrolysis enhancement and enzyme recovery

Figure 7a shows the MCC hydrolysis yield by cellulase immobilized on ZIF-8-NH$_2$ and Fe$_3$O$_4$@ZIF-8-NH$_2$,

compared to free cellulase, under the condition of 5 FPU/g enzyme dosage. It was observed that the hydrolysis yields of the immobilized cellulases are higher than that of the free enzyme. The yield using free cellulase was 51.99%, while yields for cellulases immobilized on ZIF-8-NH$_2$ and Fe$_3$O$_4$@ZIF-8-NH$_2$ were 68.41% and 71.44%, respectively. Additionally, Fe$_3$O$_4$ nanoparticles provide extra surface area and binding sites for enzyme immobilization, leading to higher enzyme loading and consequently higher hydrolysis yields.
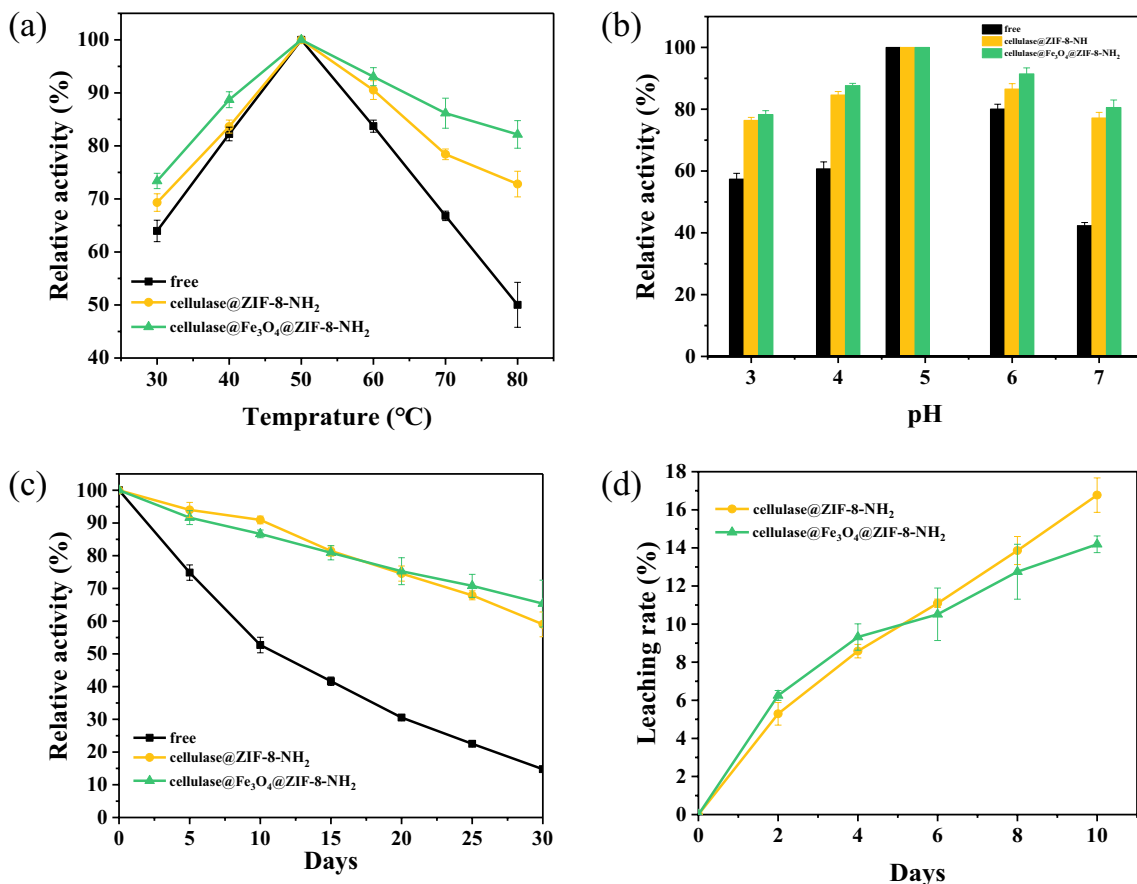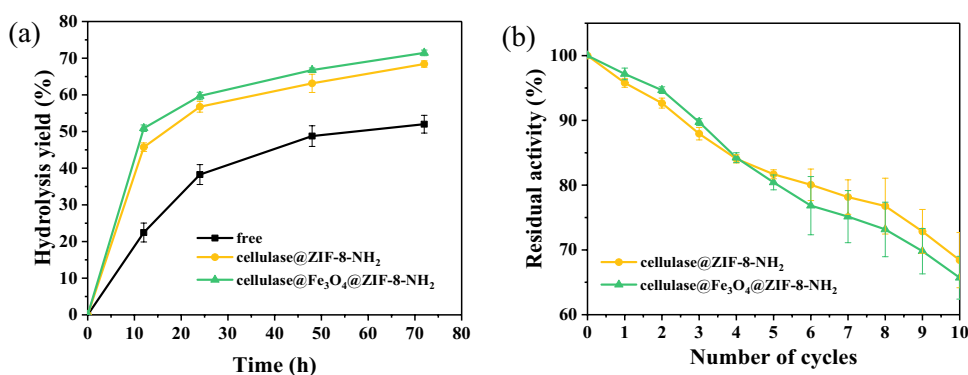

Fig. 6 **a** Temperature stability, **b** pH stability, **c** storage stability and **d** leaching test of free and ZIF-immobilized cellulases

Fig. 7 Cellulose hydrolysis yields and the residual activities after multiple cycles using different ZIF-immobilized cellulases

A key objective of immobilizing cellulase on carriers is to enable the recycling of this high-cost enzyme. As shown in Fig. 7b, this study evaluated the recyclability of immobilized cellulase over 10 consecutive cycles. After 10 cycles, the cellulase immobilized on ZIF-8-NH$_2$ retained 65.71% of its original activity, while the enzyme immobilized on Fe$_3$O$_4$@ZIF-8-NH$_2$ maintained 68.42% activity. This indicates that immobilization not only enhances enzyme efficiency, but also significantly improves its reusability, making the process more cost-effective and sustainable [25]. Additionally, compared to ZIF-8-NH$_2$, Fe$_3$O$_4$@ZIF-8-NH$_2$ contains magnetic nanoparticles, allowing for its recovery using an external magnetic field. This method significantly reduces process time and costs compared to centrifugation or filtration, and facilitates the recovery and reuse of the enzyme. Figure 8a and b show photos of cellulase@Fe$_3$O$_4$@ZIF-8-NH$_2$ in buffer before and after the application of an external magnetic field. It is evident that the introduction of an external magnetic field allows for the easy recovery of cellulase@Fe$_3$O$_4$@ZIF-8-NH$_2$.
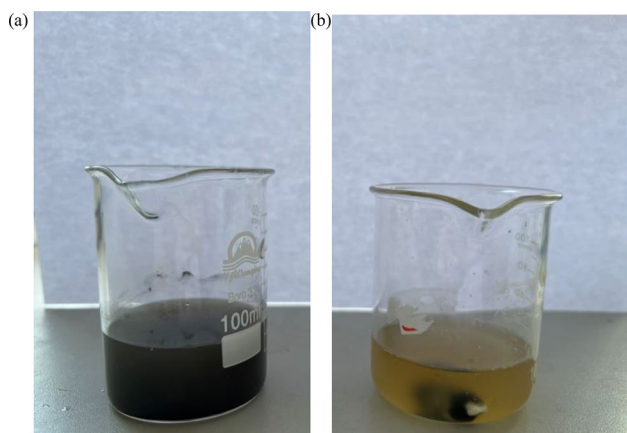
Comparative study of immobilization efficiency and reusability by various MOF supports

Figure 9 summarizes the enzyme loading capacity and reusability achieved by immobilizing cellulase on various MOF supports. The enzyme loading capacities of the two ZIF supports investigated in this research exceeded most of the previous studies, reaching 263.38 mg/g and 339.64 mg/g, respectively. Furthermore, the residual enzyme activity after 5 cycles of reuse in this study reached 82.43% and 85.14%, also surpassing most of the prior research. It is noteworthy that, compared to our previous study [24] where cellulase was immobilized using the cross-linking method (with a loading of 359.89 mg/g), this research demonstrates a relatively lower enzyme loading. However, the activity of 71.39% surpasses the previous 69.35%. This improvement is speculated to be due to the use of glutaraldehyde as a cross-linking agent, which can effectively increase the loading of cellulase on
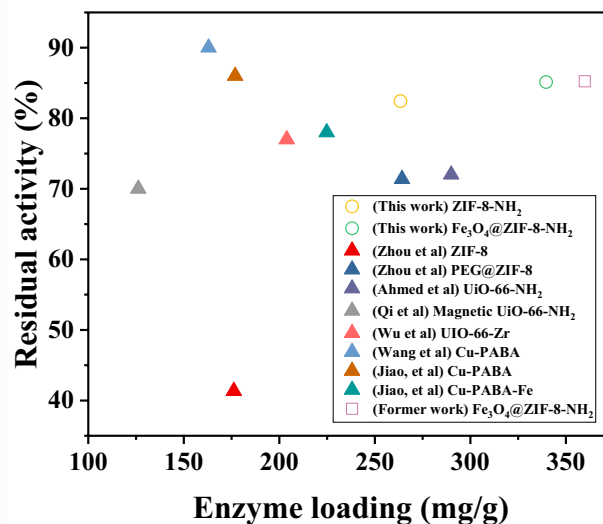

Fig. 8 a Photo of cellulase@Fe$_3$O$_4$@ZIF-8-NH$_2$ in the buffer before the introduction of an external magnetic field, **b** Photo of cellulase@Fe$_3$O$_4$@ZIF-8-NH$_2$ in the buffer after the introduction of an external magnetic field

Fig. 9 Comparative study of immobilization efficiency and reusability by different MOF-immobilized cellulases after 5 cycles [8, 9, 19, 26–31]

ZIF-8. Nonetheless, glutaraldehyde may have a certain toxic effect on cellulase itself, leading to partial deactivation and thus reducing the hydrolysis yield. Moreover, the adsorption method is simpler and more cost-effective than the cross-linking method. Consequently, the immobilized cellulase supports and methodologies developed in this study significantly enhanced the enzyme loading capacity and reusability, highlighting the advantages over previous research efforts.

Conclusion

The study successfully demonstrates the enhanced thermal, pH, and storage stability of cellulase when immobilized on ZIF-8-NH$_2$ and Fe$_3$O$_4$@ZIF-8-NH$_2$ carriers. The immobilized enzymes showed superior hydrolysis efficiency compared to free enzymes and maintained significant activity over multiple usage cycles. These findings underscore the potential of using ZIF-based immobilization for cellulase in industrial applications, offering a more sustainable and cost-effective approach to biomass hydrolysis. Future work could explore the scalability of this method and its applicability to other industrially relevant enzymes.

Data availability Data are provided within the manuscript or supplementary information and the other data will be made available on request.

Declarations

References

1. Raj T, Chandrasekhar K, Kumar AN, Banu JR, Yoon J, Bhatia SK, Yang Y, Varjani S, Kim S (2022) Recent advances in commercial biorefineries for lignocellulosic ethanol production: current status, challenges and future perspectives. Bioresource Technol 344:126292

2. Dong C, Patel AK, Madhavan A, Chen C, Singhania RR (2023) Significance of glycans in cellulolytic enzymes for lignocellulosic biorefinery—a review. Bioresource Technol 379:128992

3. Xu C, Tong S, Sun L, Gu X (2023) Cellulase immobilization to enhance enzymatic hydrolysis of lignocellulosic biomass: an all-inclusive review. Carbohyd Polym 321:121319

4. Lima JS, Araujo PHH, Sayer C, Souza AAU, Viegas AC, de Oliveira D (2017) Cellulase immobilization on magnetic nanoparticles encapsulated in polymer nanospheres. Bioproc Biosyst Eng 40:511–518

5. Andriani D, Sunwoo C, Ryu H, Prasetya B, Park D (2012) Immobilization of cellulase from newly isolated strain bacillus subtilis td6 using calcium alginate as a support material. Bioproc Biosyst Eng 35:29–33

6. de Souza Lima J, Immich APS, de Araujo PHH, de Oliveira D (2022) Cellulase immobilized on kaolin as a potential approach to improve the quality of knitted fabric. Bioproc Biosyst Eng 45:679–688

7. Ungurean M, Paul C, Peter F (2013) Cellulase immobilized by sol - gel entrapment for efficient hydrolysis of cellulose. Bioproc Biosyst Eng 36:1327–1338

8. Ahmed IN, Yang X, Dubale AA, Li R, Ma Y, Wang L, Hou G, Guan R, Xie M (2018) Hydrolysis of cellulose using cellulase physically immobilized on highly stable zirconium based metal-organic frameworks. Bioresource Technol 270:377–382

9. Qi B, Luo J, Wan Y (2018) Immobilization of cellulase on a core-shell structured metal-organic framework composites : better inhibitors tolerance and easier recycling. Bioresource Technol 268:577–582

10. Xu L, Geng X, Li Q, Li M, Chen S, Liu X, Dai X, Zhu X, Wang X, Suo H (2024) Calcium-based mofs as scaffolds for shielding immobilized lipase and enhancing its stability. Colloids Surf, B 237:113836

11. Suo H, Qi Q, Dai X, Geng X, Li Q, Yang J, Liu G, Liu R, Xu L (2023) Metal–organic framework-supported ionic liquids for lipase immobilization: design, characterization, and investigation of catalytic performance. React Chem Eng 8:2365–2374

12. Shen X, Du Y, Du Z, Tang X, Li P, Cheng J, Yan R, Cui J (2023) Construction of enzyme@glutathione hybrid metal-organic frameworks: glutathione-boosted microenvironment fine-tuning of biomimetic immobilization for improving catalytic performance. Mater Today Chem 27:101326

13. Du Y, Jia X, Zhong L, Jiao Y, Zhang Z, Wang Z, Feng Y, Bilal M, Cui J, Jia S (2022) Metal-organic frameworks with different dimensionalities: an ideal host platform for enzyme@mof composites. Coordin Chem Rev 454:214327

14. Wang Z, Wang R, Geng Z, Luo X, Jia J, Pang S, Fan X, Bilal M, Cui J (2023) Enzyme hybrid nanoflowers and enzyme@metal–organic frameworks composites: fascinating hybrid nanobiocatalysts. Crit Rev Biotechnol. https://doi.org/10.1080/07388551.2023.2280755

15. Du Y, Gao J, Zhou L, Ma L, He Y, Zheng X, Huang Z, Jiang Y (2019) Mof-based nanotubes to hollow nanospheres through protein-induced soft-templating pathways. Adv Sci 6:1801684

16. Liu J, Sun Z, Deng Y, Zou Y, Li C, Guo X, Xiong L, Gao Y, Li F, Zhao D (2009) Highly water-dispersible biocompatible magnetite particles with low cytotoxicity stabilized by citrate groups. Angew Chem Int Edit 48:5875–5879

17. Bradford MM (1976) A rapid and sensitive method for the quantitation quantities microgram principle of protein-dye binding. Anal Biochem 72:248–254

18. GHOSE, T. K. (1987) Measurement of cellulase activities. Pure Appl Chem 2:257–268

19. Xu C, Sun L, Tong S, Ouyang J, Gu X (2023) Cellulase immobilization on zeolitic imidazolate frameworks for boosting cellulose hydrolysis at high solids loading. Ind Crop Prod 206:117693

20. Cheong L, Wei Y, Wang H, Wang Z, Su X, Shen C (2017) Facile fabrication of a stable and recyclable lipase @ amine-functionalized zif-8 nanoparticles for esters hydrolysis and transesterification. J Nanopart Res. https://doi.org/10.1007/s11051-017-3979-3

21. Cheng Z, Z. S. F. W. (2023) Environmental functional materials. Environm Funct Mater. 2:36–45

22. Chen BY, Qiu J, Mo H, Yu Y, Ito K, Sakai E, Feng HX (2017) Synthesis of mesoporous silica with different pore size for cellulase immobilization: pure physical adsorption. New J Chem 41:9338–9345

23. Binhayeeding N, Yunu T, Pichid N, Klomklao S, Sangkharak K (2020) Immobilisation of candida rugosa lipase on polyhydroxybutyrate via a combination of adsorption and cross-linking agents to enhance acylglycerol production. Process Biochem 95:174–185

24. Ahmed Z, Arshad A, Bilal M, Iqbal HMN, Ahmed I (2023) Nano-biocatalytic systems for cellulose de-polymerization : a drive from design to applications. Top Catal 66:592–605

25. Cheng Z, Sun Z, Wei F, Yu J, Zhao J, Chen J, Wang J, Zhang Y (2023) Immobilization of the crude enzyme extracted from stenotrophomonas sp. Gyh within modified zeolitic imidazolate framework (zif-8-nh2) and its application in trichloromethane removal. Environ Funct Mater 1:36–45

26. Zhou M, Ju X, Zhou Z, Yan L, Chen J, Yao X, Xu X, Li L (2019) Development of an immobilized cellulase system based on metal—organic frameworks for improving ionic liquid tolerance and in situ saccharification of bagasse. ACS Sustain Chem Eng 7:19185–19193

27. Zhou M, Yan L, Chen H, Ju X, Zhou Z, Li L (2021) Development of functionalized metal—organic frameworks immobilized cellulase with enhanced tolerance of aqueous-ionic liquid media for in situ saccharification of bagasse. Fuel 304:121484

28. Wu J, Wang Y, Han J, Wang L, Li C, Mao Y, Wang Y (2022) A method of preparing mesoporous zr-based mof and application in enhancing immobilization of cellulase on carrier surface. Biochem Eng J 180:108342

29. Wang L, Zhi W, Wan J, Han J, Li C, Wang Y (2019) Recyclable beta-glucosidase by one-pot encapsulation with cu-mofs for enhanced hydrolysis of cellulose to glucose. ACS Sustain Chem Eng 7:3339–3348

30. Jiao R, Wang Y, Pang Y, Yang D, Li Z, Lou H, Qiu X (2023) Construction of macroporous β-glucosidase@mofs by a metal competitive coordination and oxidation strategy for efficient cellulose conversion at 120 °C. ACS Appl Mater Inter 15:8157–8168

31. Jiao R, Pang Y, Yang D, Li Z, Lou H (2022) Boosting hydrolysis of cellulose at high temperature by beta-glucosidase induced metal-organic framework in-situ co-precipitation encapsulation. Chemsuschem 15:202201354